Journal of Applied Polymer Science

Preparation of Chitosan-g-Poly(acrylamide)/Montmorillonite Superabsorbent Polymer Composites: Studies on Swelling, Thermal, and Antibacterial Properties

Hafida Ferfera-Harrar, Nacera Aiouaz, Nassima Dairi, Assia Siham Hadj-Hamou
Materials Polymer Laboratory, Department of Macromolecular Chemistry, Faculty of Chemistry, University of Sciences and Technology Houari Boumediene USTHB, B.P. 32 El-Alia, 16111, Algiers, Algeria.
Correspondence to: H. Ferfera-Harrar (E-mail; harrarhafida@yahoo.fr)

ABSTRACT: Superabsorbent composites based on chitosan-g-poly(acrylamide) and montorillonite (CTS-*g*-PAAm/MMT) were synthesized through *in situ* radical polymerization by grafting of crosslinked acrylamide onto chitosan backbone in presence of MMT at different contents. The formation of the grafted network was confirmed by attenuated total reflectance Fourier transform infrared spectroscopy (ATR-FTIR), thermogravimetric analysis (TGA), and differential scanning calorimetery (DSC). The obtained porous structure was observed by scanning electron microscope (SEM). The presence of clay and its interaction with chitosan-*g*-poly(acrylamide) (CTS-*g*-PAAm) matrix was evidenced by ATR-FTIR analysis. The morphology was investigated by both X-ray diffraction (XRD) and SEM analyses. It was suggested the formation of mostly exfoliated structures with more porous structures. Besides, the thermal stability of these composites, observed by TGA analysis, was slightly affected by the clay loading as compared to the matrix. These hydrogel composites were also hydrolyzed to achieve anionic hydrogels with ampholytic properties. Swelling behaviors were examined in doubly distilled water, 0.9 wt % NaCl solution and buffer solutions. The water absorbency of all superabsorbent composites was enhanced by adding clay, where the maximum was reached at 5 wt % of MMT. Their hydrolysis has not only greatly optimized their absorption capacity but also improved their swelling rate and salt-resistant ability. The hydrolyzed superabsorbent showed better pH-sensitivity than the unhydrolyzed counterparts. The results of the antibacterial activity of these superabsorbents composites against Staphylococcus aureus (*S. aureus*) and *Escherichia coli* (*E. coli*), assayed by the inhibitory zone tests, have showed moderate inhibition of the bacteria growth. © 2013 Wiley Periodicals, Inc. J. Appl. Polym. Sci. **2014**, *131*, 39747.

KEYWORDS: composites; polysaccharides; clay; crosslinking; grafting

Received 10 April 2013; accepted 9 July 2013
DOI: 10.1002/app.39747

INTRODUCTION

Superabsorbent polymers (SAPs) are crosslinked three-dimensional network characterized by their hydrophilicity and insolubility in water. They are basically the materials that can absorb fluids of >15 times their own dried weight, either under load or without load, such as water, electrolyte solution, synthetic urine, brines and biological fluids like blood. This hydrophilicity is due to the presence of water soluble groups such as carboxylic acid, amine, hydroxyl, carboxamide, and imide. The majority of them are responsive to environmental stimulants such as pH, ionic strength, solvent composition, electrical field, and irradiation. This is the reason that these gels are occasionally referred to as responsive, stimuli-sensitive, and intelligent or smart.[1,2] Owing to the excellent properties, the use of the SAPs is steadily increasing and their applications are continuing to grow such as in hygienic products and bio-related uses (mostly disposable diapers, feminine napkins), agriculture and horticulture (e.g., water reserving in soil and controlled release of agrochemicals), wastewater treatment, drug-delivery systems, absorbent pads and other special fields.[3,4] However, most of these superabsorbents are based on synthetic polymers, such as acrylic acid and acrylamide, which are poor in biodegradability with potential for inherent environmental issues. Incorporation of biodegradable and renewable polymers is a convenient way to improve biodegradability of corresponding superabsorbent materials. Thus, the development of eco-friendly natural-based super swelling hydrogels has drawn much interest owing to their abundant resources, low production cost and biodegradability. Hydrogels based on totally/partially renewable polymers are classified into polysaccharide and poly(amino acid)-based kinds. The polysaccharide-based hydrogels are usually studied, so that the term natural-based hydrogel often implies the hydrogel with carbohydrate polymer component.

Great attention has been directed toward superabsorbent polymers being prepared through graft copolymerization of vinyl monomers onto natural polymer chains such as starch,[5] cellulose,[6] and chitosan.[7] The chitosan (CTS), a copolymer of *N*-acetyl-glucosamine and *N*-glucosamine units distributed randomly or in blocks throughout its chains, is the second most abundant natural polymers after cellulose in the world. It has several interesting properties, such as gel and film forming ability, bioadhesion, biodegradability and biocompatibility. In addition, CTS antimicrobial activities against a variety of bactericides and fungi are well known and affected by many factors such as molecular weight, pH value, and water solubility.[8,9] So, superabsorbents including CTS may possess antibacterial activity and thus could be used in hygienic appliances (infant diapers, feminine hygiene products, sanitary napkins, sponges, surgical pads, …) and other special fields.[10]

Also, the reactive NH_2 and OH groups of CTS are convenient for graft copolymerization of vinyl monomers, making it an efficient way to acquire hydrogels with novel properties.

In this context, graft copolymerization of acrylamide (AAm), which forms hydrogels with attractive swelling capacity, onto CTS backbones and networking not only could improve biodegradability of its corresponding superabsorbent materials but also reduces dependence on petrochemical-derived monomers. Furthermore, the hydrolysis of crosslinked poly(acrylamide) (PAAm), in where some amide groups are converted to carboxylate anions, is expected to lead to hydrogel with ampholytic properties.

Besides, many efforts have been made to improve mechanical strength and toughness of hydrogels by adding inorganic particles into matrix or forming interpenetrating network (IPN).[11,12]

Clays were widely used in the preparation of superabsorbent polymer composites (SAPCs) due to their availability, inexpensiveness and hydrophilic nature. They often improve the mechanical and swelling properties and reduce production cost of corresponding superabsorbents.

Several clays such as kaolin,[13] mica,[14] attapulgite,[15] vermiculite,[16] sepiolite,[17] and montmorillonite[18] have so far been used in the syntheses of SAPCs that combine elasticity and permeability of the gel with high ability of the clay to adsorb different substances. Among them, the montmorillonite (MMT), a non toxic layered silicate with exchangeable cations and reactive OH groups on its layers surfaces, is the most used owing to its high in plane strength, stiffness, and high aspect ratio.[19]

In the present work, we first prepared a series of chitosan-*g*-poly(acrylamide)/montmorillonite (CTS-*g*-PAAm/MMT) superabsorbent composites at different clay contents, with the aim to elaborate superabsorbent materials with enhanced properties, such as swelling capacity, thermal resistance, biodegradability and antibacterial activity. Then, we reported on their characterization by different techniques (ATR-FTIR, XRD, SEM, DSC and TGA) and we studied the effect of MMT loading on their morphology and thermal properties. Also, we partially hydrolyzed the elaborated hydrogels, and then we focused our study on the influence of clay contents and hydrolysis treatment on the swelling capacities of unhydrolyzed and hydrolyzed composites in various aqueous media (doubly distilled water, NaCl 0.9 wt % and buffer solutions) and compared to those of the CTS-g-PAAm matrix. Finally, antibacterial activity of these composites against Gram-positive bacteria *Staphylococcus aureus (S. aureus)* and Gram-negative bacteria *Escherichia coli* (*E. coli*) was investigated by zone inhibition method.

To our knowledge, the elaboration of such materials using the grafted network CTS-g-PAAm as matrix and a montmorillonite, originated from Maghnia bentonite in Algeria, as nanofiller has not been reported in the literature yet.

EXPERIMENTAL

Materials

Chitosan (CTS, from Sigma–Aldrich, 75% degree of deacetylation and medium average molecular weight, viscosity 200–800 cps), Acrylamide (AAm, from Fluka), *N*,*N*′-methylenebisacrylamide (MBA, from Merck) and potassium persulfate (KPS, from Fluka) were used as received. All other chemicals were of analytical grade. Doubly distilled water was used for hydrogels preparation and swelling measurements.

The clay used in this study was an Algerian montmorillonite (MMT), a bentonite category from Roussel in Maghnia that was kindly supplied by ENOF Chemical, Research Company of "non ferreux," Algeria. The montmorillonite (size fraction < 2 μm) was extracted from bentonite using the sedimentation method.[20] It was homoionized with sodium cations (Na-MMT) and then the cation exchange capacity (CEC) was determined about 86.16 mmol/100 g by conductometric titration.[21]

The bacteria *Staphylococcus aureus* (ATCC 25923) and *Escherichia coli* (ATCC 25922) were kindly obtained from Microbiology Laboratory of Bejaia city University, Algeria.

A series of CTS-*g*-PAAm/MMT superabsorbent polymer composites were prepared at various clay contents via *in situ* intercalative radical graft-copolymerization and crosslinking at 60°C in aqueous solution. The weight ratios of CTS, KPS, and MBA with respect to AAm were kept constant in all experiments, while clay content was varied (2, 5, 10 and 15 wt %). In typical procedure: 1 g (20 wt %) of CTS was dissolved in 30 mL 1% (v/v) acetic acid solution in a 250 mL three-necked flask, equipped with a reflux condenser, a funnel, a nitrogen line and a magnetic stirrer. After being purged with nitrogen to remove the dissolved oxygen, the flask was placed in water bath preset at 60°C for 30 min. Then 0.1 g (2 wt %) of KPS was added to the CTS solution and the resulting mixture was gently stirred for an additional 15 min (delay time) at 60°C to generate radicals. In the other hand, a required amount of Na-MMT was previously suspended in 40 mL of doubly distilled water and allowed to swell at room temperature for 24 h under vigorous mechanical stirring. Following this, the clay suspension was ultrasonically pretreated for 30 min and was added to 30 mL of the aqueous mixed solution of AAm (5g, 7×10^{-2} mol) and MBA (0.05 g, 1 wt %) then kept under stirring at room temperature for 30 min. Subsequently, the mixture was introduced into the funnel and degassed for 15 min, and then added to the flask. The solution was stirred vigorously for another 3 h and a

nitrogen atmosphere was maintained all through the polymerization.

Next, the resulting hydrogel was allowed to cool to ambient temperature and neutralized to pH 8 by adding 1*N* NaOH solution.

The swollen products were immersed in an excess of doubly distilled water, washed repeatedly and then dewatered with 500 mL of methanol for 24 h. After complete dewatering, the gel particles were filtered, washed with methanol (2 × 50 mL) and dried in an oven at 70°C to a constant weight. Finally, the product was ground (particles size in the range of 40–60 mesh) and stored away from moisture, heat and light.

Apart from the omission of clay, the preparation method of CTS-*g*-PAAm superabsorbent was similar to that of CTS-*g*-PAAm/MMT superabsorbent composite. The crosslinked single PAAm (without CTS) was prepared according to the same procedure.

The partial hydrolysis of crosslinked CTS-*g*-PAAm and its Na-MMT composites was carried out in alkaline medium. About 0.50 g of each dried hydrogel was introduced in 100-mL flask and hydrolyzed at 95°C using 20 mL of 1*N* NaOH solution. After 2 h, the obtained product was allowed to cool to ambient temperature and neutralized to pH 8 by adding acetic acid solution (10 wt %). Following a complete dewatering by methanol (200 mL), the yellow product was filtered, washed with fresh methanol (2 × 50 mL) and dried in an oven at 50°C.

Characterizations

ATR-FTIR spectra were performed on Bio-Rad (Inc., USA) spectrometer model FTS-162.

Samples of hydrogels and clay were analyzed in solid state, without any preliminary preparation, as small grains and powder, respectively.

X-ray diffractograms of pristine Na-MMT, grafted network CTS-g-PAAm and its composites were recorded with a D8 advance diffractometer (Bruker, Germany) using Cu Kα monochromatic radiation (40 kV, $\lambda = 1.5406$ Å) in 2θ range 1–30° with 0.01° s^{-1} scan rate.

To study the surface morphology of these hydrogels, the cross-sectioned surface area of each dried sample was examined on JSM-6360LV Scanning Electron Microscope (JEOL, USA) after its coating with gold film using an acceleration voltage of 10 kV.

Thermal stability of these superabsorbents was investigated using TGA analysis. The measurements were performed on a Q500 analyzer, TA instruments, at a heating rate of 10°C min^{-1}, under nitrogen atmosphere from 30 to 600°C.

DSC analysis was recorded on a Q100, TA instruments. Special care must be taken during analysis since hydrogels are apt to absorb moisture, which should strongly affect the measurements. Thus, two cycles of heating and cooling runs were adopted in the temperature ranges 30–160°C and 30–240°C, under nitrogen flow at 10°C min^{-1}. Glass transition temperature (T_g) was determined at the mid-point of the glass transition after the second scan.

Swelling Measurements in Various Swelling Media

Swelling capacities of the CTS-*g*-PAAm superabsorbent and its MMT composites were gravimetrically studied in doubly distilled water and in saline solution of NaCl 0.9 wt %. Because these measurements were continued up to 48 h and to avoid the fluctuations of the room temperature (18–27°C), which may affect the swelling results, the temperature value was controlled by introducing the flasks samples into a thermostated water bath at 25°C.

An accurately weighed sample (0.1 g) was immersed in excess swelling solvent (500 mL), and allowed to soak at room temperature to reach swelling equilibrium. The swollen sample was separated from unabsorbed water by filtering through an 80-mesh stainless steel screen and drained for 30 min until no free water remained. The water absorbency (swelling equilibrium ratio), Q_{eq}, was calculated, as grams of water per gram of sample, by weighing the fully swollen hydrogel using eq. (1). All tests were carried out three times repeatedly and the average values were reported.

$$Q_{eq}\,(g/g) = \frac{W_s - W_d}{W_d} \quad (1)$$

where W_d and W_s are the sample's weights in the dry and the swollen states, respectively.

Water absorbency of the superabsorbing composites was also examined in buffer solutions with pH ranging from 3 to 10. The pH values were precisely checked by a pH-meter type Metrohm/620.

About 0.1 g of dried sample was immersed in each buffer medium to reach equilibrium swelling according to the previously mentioned method.

Comparative swelling study of partially hydrolyzed hydrogels composites was also carried out in water, NaCl 0.9 wt % and buffer solutions.

Swelling rate, Q_t, of the grafted superabsorbent and its MMT composites was measured in water, before and after hydrolysis. In brief, a weighted (0.04 g) piece of each sample was immersed in an amount of water, taken out at desired time intervals, and then the weight of the swollen sample was measured against time after wiping off the excessive water by gently tapping the surface with a wet filter. The swelling capacity was evaluated similarly to the above method.

Antibacterial Activity Tests

Antibacterial activity of the grafted hydrogel CTS-*g*-PAAm and its MMT composites at different clay loadings was tested against both bacteria *S. aureus* and *E. coli*, using inhibition zone method.

The nutrient broth was used as a preserving medium for the microorganisms at 6°C. The bacteria were incubated overnight at 37°C. Then, individual colonies were isolated and suspended in 0.9% NaCl solution to reach 10^6 CFU mL^{-1}. The inhibitory zone tests were performed in Müller Hinton Agar into sterilized

Petri plates that were streaked with the bacterial suspension. Otherwise, all hydrogels were sterilized in an autoclave at 120°C for 20 min and swollen in distilled water or acetic acid solution (0.5% w/w) media. After 24 h, the obtained samples were cut into disks (5-mm diameter), placed over the surface of the agar plates and then incubated at 37°C for 24 h.

The antibacterial activity of the materials was evidenced by the appearance of inhibitory zones.

RESULTS AND DISCUSSION

Evidences for the Formation of the Grafted Network

ATR-FTIR spectra of crosslinked PAAm, CTS and grafted network are presented in Figure 1. As it can be seen, PAAm spectrum displays mainly broad bands around 3333 and 3186 cm^{-1} due to asymmetric and symmetric stretching vibrations of N—H, respectively. The bands at 1645, 1600, and 1414 cm^{-1} are ascribed to $\nu_{C=O}$ (amide I), δ_{N-H} (amide II), and ν_{C-N} (amide III), respectively.[22]

In the spectrum of CTS, the absorption bands at 1657, 1598, 1379 and 1320 cm^{-1} are assigned to $\nu_{C=O}$ (amide I) of acetyl groups, δ_{N-H} of NH_2 and NHCO groups, δ_{CO-NH} (amide III) and in plan δ_{O-H} of hydroxyl groups. The band observed at 1158 cm^{-1} and the strong one in 1190–1000 cm^{-1} region that is centered at 1080 cm^{-1} are attributed to C—O stretching vibrations in alcohols (ν_{C-OH}) and in anhydroglucose units (skeletal ν_{C-O-C}), respectively.[22,23]

In the grafted CTS-*g*-PAAm spectrum, both components have the most of their characteristic bands in the same regions, so it is difficult to assign precisely the bands and to get a clear image about their structural features. Only an additional large band characteristic of CTS can be detected in a region non disturbed by PAAm bands near 1080 cm^{-1} that is due to ν_{C-O-C} of piranose ring.

Therefore, the presence of AAm together CTS in the network suggests that the grafting of AAm onto CTS backbone containing radical active sites, which were previously generated by the action of KPS as initiator, has most likely taken place. The growth of PAAm chains on CTS macroradicals and crosslinking leads to the formation of CTS-*g*-PAAm grafted network.

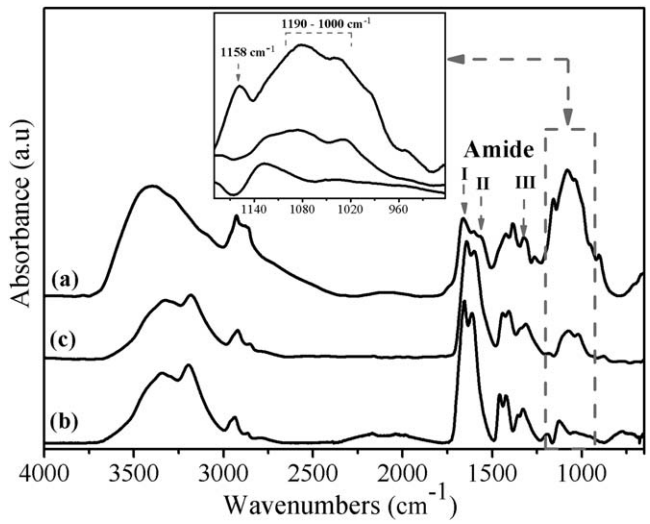

Figure 1. ATR-FTIR spectra of (a) CTS, (b) PAAm hydrogel and (c) the grafted networkCTS-*g*-PAAm.

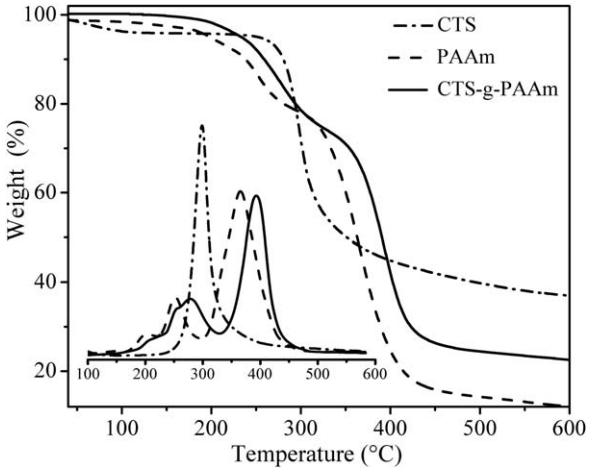

Figure 2. TGA and d(TG) curves of CTS, PAAm hydrogel and the grafted network CTS-*g*-PAAm.

The graft-copolymerization of AAm onto CTS backbones can also be supported by TGA analysis. Figure 2 shows TGA and d(TG) curves of CTS, crosslinked PAAm and CTS-*g*-PAAm network.

As illustrated in TGA and d(TG) curves of CTS, besides the weight loss up to 120°C, due to adsorbed and bound water, the thermal degradation of CTS occurs mainly in one step, between 218 and 500°C which is initiated by the random chains breaking and deacetylation reactions.[24]

The maximal decomposition temperature (Td_{max}) is observed at 298°C.

The curves of PAAm exhibit three thermal decomposition steps. The first step occurs in the range of 150–220°C due to water loss, which is adsorbed on the surface and in the pores of the network. The second step, between 220 and 298°C, is attributed to both weight losses of NH_2 of amide side groups in ammonia form and the crosslinker.[25,26] The third one starts at 298°C and continues up to 440°C, due to entire main chain breakdown of PAAm. This main step shows about 78% weight losses and the Td_{max} is reached at 365°C.

Besides, the sample of the grafted network containing 20 wt % of CTS shows roughly similar thermal behavior as the crosslinked PAAm. The formation of the grafted hydrogel CTS-*g*-PAAm via covalent linkages is confirmed by a significant improvement in its thermal stability compared to both components of the network. The enhance in thermal resistance is evidenced by the shifting of both onset and maximum degradation temperatures (Td_{onset},Td_{max}) toward higher values as compared to PAAm and CTS. The values of both Td_{onset} and Td_{max} of CTS-*g*-PAAm are increased of about 30 and 28°C for PAAm and 100 and 95°C for CTS, respectively.

Figure 3 displays DSC curves of PAAm and CTS-*g*-PAAm hydrogel. The PAAm shows a slope change corresponding to T_g

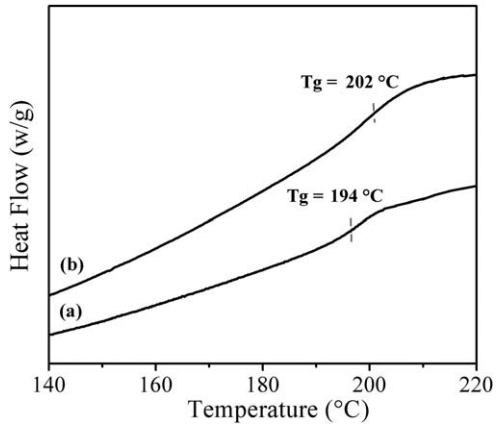

Figure 3. DSC thermograms of the hydrogels (a) PAAm and (b) CTS-*g*-PAAm.

at 194°C, while the grafted network exhibits a single transition at higher T_g at 202°C. In agreement with TGA analysis, the difference in T_g values may arise from interactions between PAAm and CTS groups through covalent and hydrogen bonding, which increase crosslinking density, and in turn reduce the sub-chain mobility of both polymers, resulting in less flexible network.[24–26] Another reason, the rigidity of the semicrystalline structure of CTS, with T_g value[27] about 203°C, which promotes the stiffness of the grafted network.

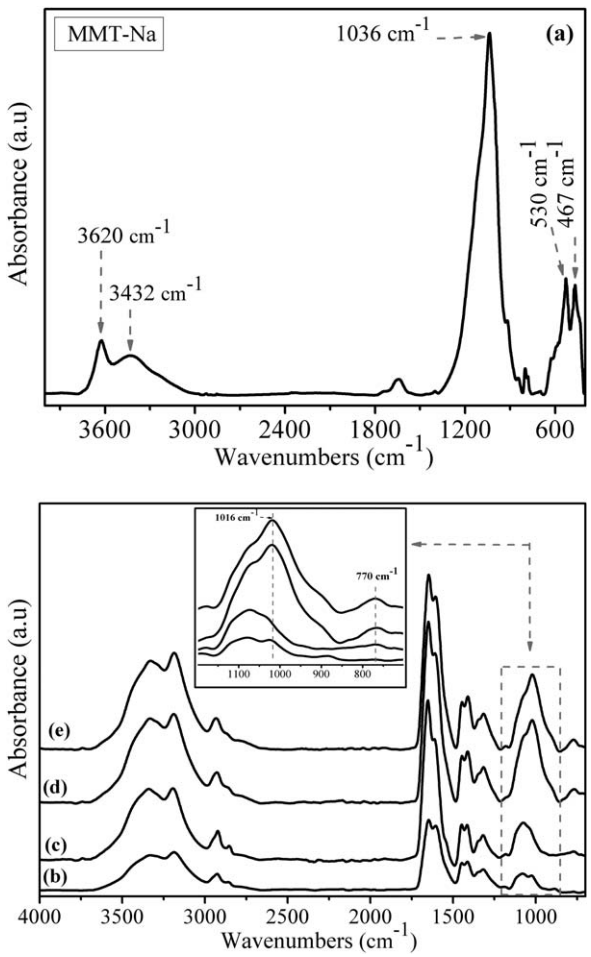

Figure 4. (a) ATR-FTIR spectrum of (a) Na-MMT. (b) ATR-FTIR spectra of (b) grafted network CTS-g-PAAm and its superabsorbent composites. MMT content (wt %): (c) 5; (d) 10; (e) 15.

According to previous studies[28,29] together with the above results of ATR-FTIR, TGA, and DSC, the most probable mechanism for the graft-copolymerization of AAm onto CTS backbones in presence of potassium persulfate as an initiator is as follows: As it is well known in literature, the thermal decomposition of persulfate ($S_2O_8^{2-}$) generates sulfate anion-radicals ($SO_4^{\cdot}$). So, these anion-radicals subsequently remove hydrogen from —OH groups of chitosan backbones and produce alkoxy radicals. These radical active centers are able to initiate the polymerization of AAm and leading to graft copolymer. Because MBA crosslinker agent is presented in the medium, the CTS-*g*-PAAm network is resulted.

Structural Study of Superabsorbent Composites by ATR-FTIR Analysis

ATR-FTIR spectra of Na-MMT, grafted CTS-*g*-PAAm and CTS-*g*-PAAm/MMT superabsorbent composites are shown in Figure 4(a,b). The Na-MMT spectrum, Figure 4(a), shows mainly the bands at 3620, 3432, 1635, 1036, 797, 530, and 467 cm^{-1} which are ascribed to the vibrations $\nu_{O—H}$ of Mg—OH and Al—OH, $\nu_{O—H}$ of H_2O, $\nu_{Si—O—Si}$, $\nu_{Si—O—Al}$, $\delta_{Si—O—Al}$ and $\delta_{Si—O—Si}$, respectively.[30]

From the spectra of CTS-*g*-PAAm/MMT composites, Figure 4(b), the incorporation of MMT into the matrix is evidenced by the appearance at 1016 cm^{-1} of its most intense characteristic band related to the stretching vibrations $\nu_{Si—O—Si}$, which is slightly overlaps by the band of the matrix at 1080 cm^{-1} resulting in a broad absorption band in the range of 850–1150 cm^{-1}. Also, this band increases in intensity with increasing clay loading in the network.

Moreover, the band of vibrations $\nu_{Si—O—Si}$, which appears at 1036 cm^{-1} in MMT spectrum, shifts to 1016 cm^{-1} in all composites spectra. Also, the absorption band of MMT at 797 cm^{-1} attributed to Si—O—Al stretching, which appears as shoulder, shifts to 770 cm^{-1} and increases in intensity as the content of clay increase. These observations suggest that the chemical environment of MMT layers has changed owing to some interactions develop between Si—O bonds of clay and the matrix groups. A similar result has been reported by other workers.[31–33] The added MMT has not caused any obvious difference in shifting or intensity variation for the other bands of the matrix, due probably to overlapping of the almost PAAm bands with those of CTS.

Through *in situ* intercalative polymerization reaction, the MMT particles can be considered as acting in one or both of two ways: (a) crosslinking agent, (b) transfer agent that prevents the growth of polymer chains by chain transfer mechanism.[34]

Evidence for Partial Hydrolysis by ATR-FTIR Analysis

To achieve superabsorbents with high swelling capacity, a portion of all synthesized superabsorbent composites were partially hydrolyzed. During this hydrolysis treatment, as illustrated in

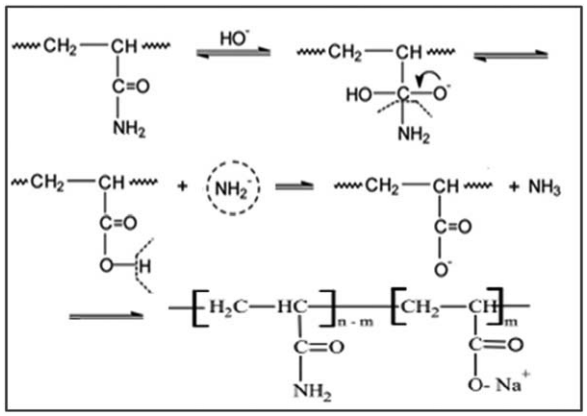

Figure 5. Schematic representation of alkaline hydrolysis mechanism of amide sides groups in polyacrylamide.

Figure 5, the carboxamide groups of PAAm are converted into carboxylate ions (COO^-) and following by the release of ammonia.

ATR-FTIR spectra of a typical composite CTS-*g*-PAAm/MMT with 10 wt % clay loading together with its hydrolyzed analogue denoted H-CTS-*g*-PAAm/MMT are shown in Figure 6.

On comparing the spectrum of hydrolyzed composite with that of unhydrolyzed one, it can be seen a strong band at 1548 cm^{-1} related to the C═O asymmetric stretching in the carboxylate anion that is confirmed by another sharp peak at 1400 cm^{-1} due to C═O symmetric stretching mode. No bands were observed at this position for the unhydrolyzed sample. In addition, the decrease in intensity of the band at 3185 cm^{-1} related mainly to N—H symmetric stretching of amide groups reveals that only some of amide groups were involved in the hydrolysis reaction. Moreover, the shifting after hydrolysis treatment of the absorption band at 1645 to 1655 cm^{-1} due to $\nu_{C=O}$ of the $CONH_2$ groups, indicates that this band develops interactions with other groups in the network. These results confirm the conversion of a part of amide groups to carboxylate salt COO^-Na^+, while hydrolyzed with NaOH.

It is interesting to mention that the partial hydrolysis in acidic medium is not a convenient way to form polyelectrolytic chains, as compared to alkaline hydrolysis, since the $CONH_2$ groups of PAAm are converted to carboxylic COOH groups. Moreover, acid hydrolysis is typically accompanied by intra- and intermolecular imidization.

Consequently, the H-CTS-*g*-PAAm/MMT structure is consisted of amide $COONH_2$, carboxylate COO^- and amine NH_2 groups, resulting in superabsorbents with ampholytic properties.

The hydrolysis degree is defined as the molar ratio of COO^- anions in the partially hydrolyzed hydrogel with respect to $CONH_2$ groups. It could be calculated using ATR-FTIR analysis by considering the absorbency ratio of both bands of carboxylate ions and amides groups, according to the formula (2).[35]

$$\text{Hydrolysis degree}\,(\%) = \frac{A_{1547}}{(A_{1547}+A_{1655})} \qquad (2)$$

The hydrolysis degrees are about 59% for the grafted network H-CTS-*g*-PAAm and its composites H-CTS-*g*-PAAm/MMT at different clay contents, in agreement with PAAm-based systems.[35,36]

X-ray Diffraction Analysis

XRD analysis is commonly used to probe the clay nanocomposites structures for its easiness and availability, by which the intercalated or exfoliated structures can be ascertained.

Figure 7 displays XRD patterns of pristine Na-MMT, grafted network CTS-*g*-PAAm and its CTS-*g*-PAAm/MMT composites with different clay contents. As can be seen, Na-MMT exhibits a sharp peak at $2\theta = 6.76°$ corresponding to a basal spacing (d_{001}) of 1.30 nm. However, in the composites diffractograms, the diffraction peak of MMT cannot be detected in low 2θ angle

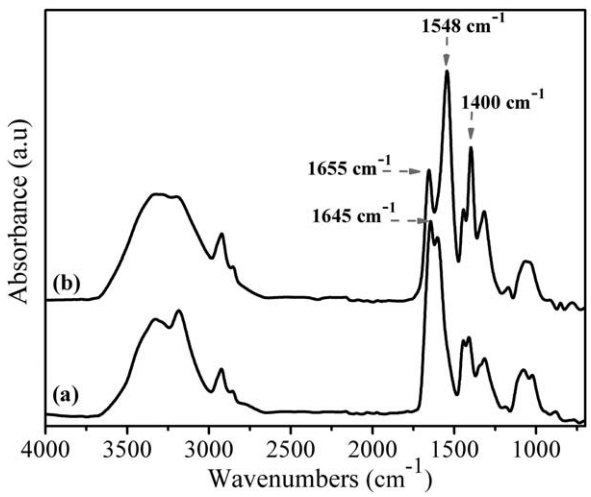

Figure 6. ATR-FTIR spectra of (a) unhydrolyzed CTS-*g*-PAAm and (b) hydrolyzed H-CTS-*g*-PAAm superabsorbent composites containing 10 wt % of MMT.

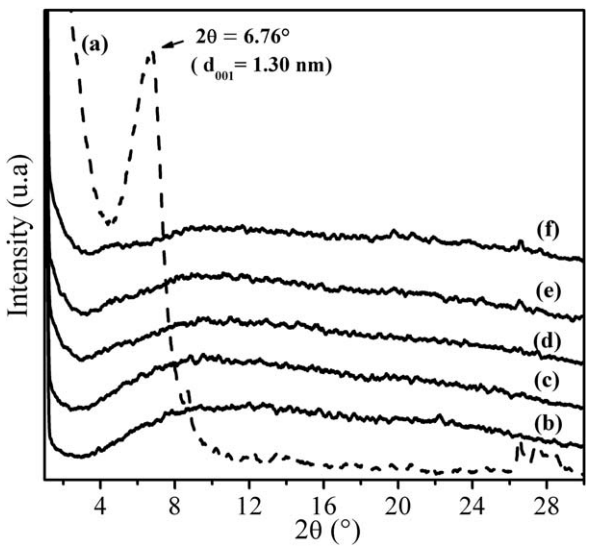

Figure 7. XRD patterns of (a) pristine Na-MMT, (b) CTS-*g*-PAAm hydrogel and its MMT composites. MMT contents: (c) 2 wt %; (d) 5 wt %; (e) 10 wt %; (f) 15 wt %.

region from 1° to 10° no matter how much clay was introduced. This result indicates that the majority of MMT platelets have been exfoliated and dispersed randomly in the matrix. In previous studies,[37] it was suggested that PAAm chains could be irreversibly absorbed into smectite layers via: (a) an ion–dipole interaction or coordination between C═O of amide groups and the exchangeable cations, (b) H-bonding between $CONH_2$ groups and water molecules in the hydration shells of exchangeable cations, and (c) hydrophobic bonding between PAAm backbone $(—CH_2—CH—)_n$ and hydrophobic basal siloxane surface Si—O—Si bands, in accord with ATR-FTIR analysis.

So, it can be propose that the reaction between PAAm chains and MMT occurs on the surface of clay and intercalating into the stacked MMT. The growth of intercalated PAAm chains provokes the exfoliation of MMT sheets. These results are in agreement with Wang et al. studies reported on superabsorbent composites based on poly(acrylamide) incorporated with MMT and vermiculite[38] as well as on chitosan-*g*-poly(acrylic acid)/clay systems.[31,39,40] Furthermore, these authors[31,40] have concluded that in systems based on chitosan-*g*-poly(acrylic acid), the exfoliation of clay platelets is most likely attributed to the fact that CTS could first intercalate into MMT layers, and then formed the composite through graft-copolymerization with AAm. Indeed, it is well established that in acidic diluted medium the protonated CTS chains rich in NH_3^+ exhibit an extended structure that facilitates their intercalation between the layers of silicate via cation-exchange process.[41] In fact, the electrostatic interactions between the positive $—NH_3^+$ groups of chitosan with the negatively charged sites of clay layers surfaces produce the substitution of the starting Na^+ cations into interlayers spaces of MMT.

Morphological Study by SEM Analysis

The porosity of the hydrogels plays multiple role of enhancing the total water sorption capability and the rate of response by reducing the transport resistance. Hence, one of the most important properties that must be considered is hydrogel structure. SEM micrographs of CTS, grafted network CTS-g-PAAm and typical CTS-*g*-PAAm/MMT superabsorbent composites with 10 and 15 wt % clay loadings were observed and are shown in Figure 8.

CTS-*g*-PAAm exhibits porous structure, Figure 8(b–d), though no porosity is observed in the CTS structure, Figure 8(a). It is supposed that these pores are convenient for the permeation of water and are the sites for interaction of external stimuli with the hydrophilic groups of the network.

It should be mention that the dewatering method of hydrogels with organic agents that are miscible with water such as methanol has also a protection effect on their porous structure and thus enhances the water absorbency.[42,43] In fact, when methanol is added, the water is displaced from the network and the precipitated polymer retains its expanded porous structure. Also, the residual methanol is easily removed by vacuum drying, and thus the porous structure remained. In opposite, during dewatering method via oven drying, the polymer chains of the network interact with each other, which result in collapse of the porous structure, and so a decrease of water absorbency.

Obviously, the surface morphology of CTS-*g*-PAAm/MMT composites is dissimilar from that of the matrix, as shown in Figure 8(e–g). Indeed, CTS-*g*-PAAm displays a smooth and tight surface, while MMT composites show more loose porous and rough surfaces. This surface change by adding clay may be convenient for improve the water uptake in the superabsorbent composites.

In agreement with XRD findings, it is also observed that MMT layers disperse homogeneously within matrix, despite that its content reaches 15 wt %, indicating favor compatibility of inorganic and organic phases. This affinity may be promoted by hydrogen interactions between the matrix and clay hydroxyls groups.

In previous study reported by Wang et al.,[31] chitosan-*g*-poly (acrylic acid)/montmorillonite (CTS-*g*-PAA/MMT) superabsorbent composites were prepared via graft-copolymerization (designated as one-step method) and then compared to poly(-acrylic acid)/chitosan-intercalated montmorillonite (PAA/CTS-intercalated MMT) composites prepared according to two-step method, in where the MMT must be modified with CTS first, and then polymerized with acrylic acid AA to form the composites. When comparing DRX patterns of CTS-*g*-PAA/MMT composites and PAA/CTS-intercalated MMT composites, no obvious difference was found and the typical diffraction peak of MMT disappeared in both cases no matter how much the MMT was incorporated, indicating that MMT layers could be exfoliated by the two methods. Wang et al. have concluded that for CTS-*g*-PAA/MMT, under acidic conditions a part of protonated CTS could intercalate first into layers of MMT, and then the radicals on CTS would initiate the polymerization of acrylic acid and formed the exfoliated superabsorbent composite.

Therefore, on the basis of Wang et al. comparative study[31] and in view of our combined results of ATR-FTIR, XRD, and SEM analyses, the most probable formation process of CTS-*g*-PAAm/MMT superabsorbent composite, illustrates in Figure 9, is as follows: First a part of protonated CTS chains containing the radicals sites, that are generated on CTS under the existence of initiator, intercalate into MMT layers and lead to an increase in the *d*-spacing. Subsequently, these radicals initiate the graft-copolymerization of the adsorbed AAm molecules into the clay interlayer spaces, in where the growth of PAAm chains provokes exfoliation of MMT sheets.

Thermal Stability Study by TGA Analysis

The effect of MMT on thermal stability of CTS-*g*-PAAm was investigated by TGA in this section. TGA and d(TG) thermograms of CTS-*g*-PAAm hydrogel and its CTS-*g*-PAAm/MMT composites are shown and compared in Figure 10(a,b). Obviously, all composites exhibit a similar three-stage thermal degradation, within the temperature range of 30–600°C. The first stage, below 180°C, is belonging to a loss of moisture present in the samples and the second one, between 180 and 329°C, is due to both amide side groups and crosslinker. The third stage above 330°C represents substantial mass loss owing to main composite chains breakdown.

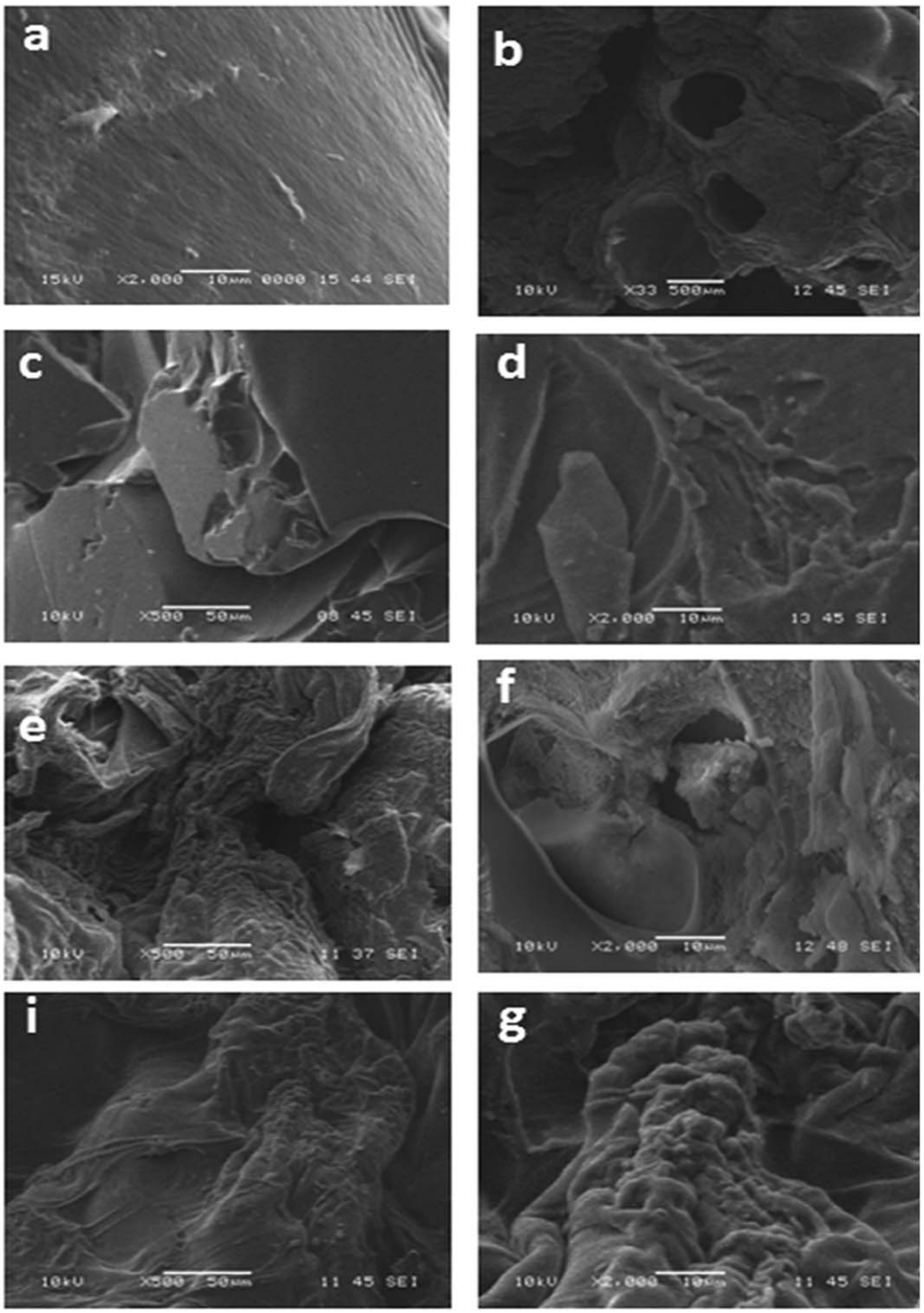

Figure 8. SEM micrographs of (a) CTS, (b–d) grafted network CTS-*g*-PAAm and CTS-*g*-PAAm/MMT superabsorbent composites. MMT contents: (e,f) 10 wt %; (i,g) 15 wt %.

Regardless clay content, it can also be seen from the inset graphs in Figure 10(a,b), which correspond to the zoom of ATG and d(TG) curves of the main degradation step, that the thermal stability is slightly enhanced as compared to that of the matrix CTS-g-PAAm, where the highest Td_{onset} and Td_{max} are greater than those of the matrix by only 5°C. The thermogravimetric data are summarized in Table I.

Also, the thermal decomposition rate within the temperature range 330–600°C is clearly reduced compared to CTS-*g*-PAAm, suggesting that addition of MMT causes a delay in matrix weight loss to a certain extent. Moreover, the char increase which acts as insulator and mass transport barrier, observed with an increase of clay loading at 586°C, also confirm the enhanced thermal stability of the elaborated composites

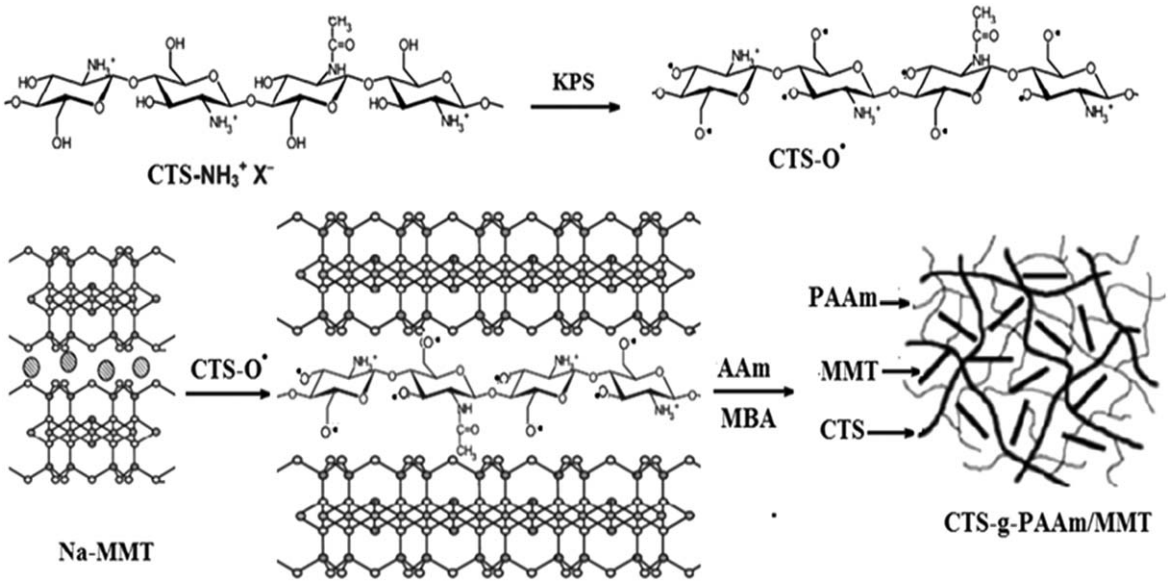

Figure 9. Mechanism of the formation of CTS-*g*-PAAm/MMT superabsorbent composite.

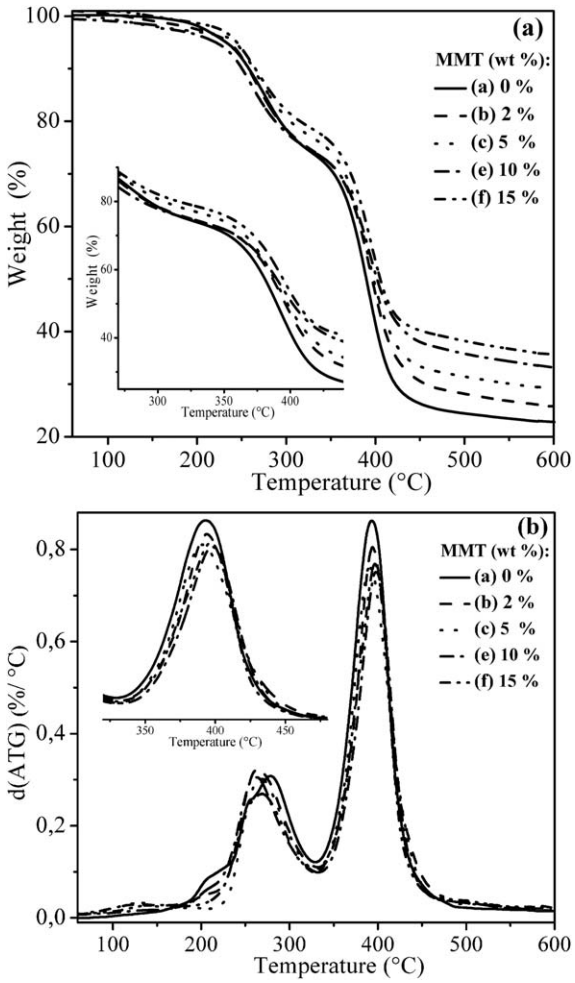

Figure 10. (a) TGA themograms of grafted CTS-*g*-PAAm hydrogel and its MMT composites. MMT contents are: 2, 5, 10, and 15 wt %. (b). d(TG) thermograms of grafted CTS-*g*-PAAm hydrogel and its MMT composites. MMT contents are: 2, 5, 10, and 15 wt %.

Table I. Thermogravimetric Parameters of CTS-g-PAAm Superabsorbent and its MMT Composites at Different Clay Loadings, Under Nitrogen Atmosphere

	Main thermal degradation (330–500°C)[a]		
Clay content (wt %)	Td_{onset} (°C)	Td_{max} (°C)	Char (%) at 586°C
0	329	393	22.82
2	331	393	26.04
5	333	392	28.38
10	334	398	32.95
15	332	396	35.16

[a] Td_{onset} is the onset degradation temperature; Td_{max} is the maximum degradation temperature.

compared to virgin matrix. This result is attributed to effects such as a decrease in permeability due to "tortuous path" effect of clay that delays the permeation of oxygen and the escape of volatile degradation products.[44] Similar clay effect on thermal resistance of hydrogel composites was also reported in literature.[32,45]

Swelling Properties in Water and Saline Solution

Some preliminary syntheses of typical CTS-*g*-PAAm/MMT superabsorbent composite were carried out by varying MBA weight ratio from 0.5 to 7 wt % while keeping the other reaction parameters constants. As expected, the swelling capacity of the hydrogel in water has decreased with an increase in MBA content. In addition, when the MBA amount was less than 0.5 wt % a slimy gel (poor dimensional stability) was formed so that the swollen gel strength is not enough to be referred to as a real superabsorbent Thus, the weight ratio of 1wt % in MBA was selected for the synthesis of all superabsorbent composites.

The effects of clay content as well as hydrolysis treatment on water absorbency of CTS-*g*-PAAm and its MMT composites are investigated in water. Also, from the view point of expanding of their applications mainly for hygienic products such as disposable diapers, it is important to study their salt-sensitivity in 0.9 wt % NaCl solution that is considered as physiological solution. Figure 11 displays water absorbency of the composites in water and NaCl 0.9 wt % solution before and after hydrolysis. It is obvious that MMT influences appreciably swelling capacity of the corresponding composites. As can be seen from curve (a), the equilibrium swelling ratios in water increases with increasing MMT loading until 5 wt %, beyond it a decrease in absorbency is observed. Similar swelling trend has been reported by other workers.[31–33,46,47]

This enhance in swelling capacity with an increase of MMT from 0 to 5 wt % can be explained by the fact that —OH group on the surface of MMT layers could react with AAm groups and create crosslinking points in the grafted network. Thus, the performance of the superabsorbent network could be improve and favor the water uptake. Moreover, MMT contains into interlayer's a lot of exchangeable Na^+ cations that are easily dispersed into the network, which enhances hydrophilicity of the composite and makes it swell more.

Further increase in MMT content, however, give arise to decrease in swelling. This may be ascribed to the fact that MMT could react increasingly with AAm owing to the increase of its —OH groups into the network.[38,40,48] Thus, at higher MMT loading additional crosslinking points are generating in the polymeric network that reduce polymer chains elasticity. Also, the content of free hydrophilic amide groups becomes lower at a higher MMT loading, which contributes to the swelling decrease.

Besides, the equilibrium swelling ratios of all composites in salt solution, shown in curve (b), decrease as compared to the values measured in water, although similar swelling trend is observed.

The optimal values for composite containing 5 wt % of MMT in water and NaCl 0.9 wt % solution are about 60 and 52 g g^{-1}, respectively. Considering that the swelling process in the network is influenced by the swelling media's ionic strength, when the ionic strength increases in the external solution, the concentration of ions in the hydrogel must increase to satisfy the Donnan osmotic pressure theory,[49] which establishes that the swelling is diminished when the interactions of the network with the counter-ions of the swelling media increase.

Figure 11, curves (c,d), illustrates also the hydrolysis effect on the swelling capacity of CTS-*g*-PAAm and its MMT composites in water and NaCl 0.9 wt % solution.

As expected, the water absorbency of hydrolyzed superabsorbents in water is remarkably higher than that of unhydrolyzed counterparts, regardless clay loading. Also, similar swelling trend is showed before and after the hydrolysis. For instance, the swelling equilibrium ratios of H-CTS-*g*-PAAm network and H-CTS-*g*-PAAm/MMT composite with 5 wt % of MMT content are about 9-fold and 7.5-fold larger than those of unhydrolyzed ones, respectively.

This significant difference in swelling capacity is ascribed to the appearance of polyelectrolytic character in these superabsorbents. Indeed, the amide groups of crosslinked PAAm chains undergo hydrolysis and this produces anionically charged polymer chains. The electrostatic repulsive forces between the anionic carboxylate (COO^-) lends to an expansion of the network chains and hence an increase in water absorbency. Besides, the presence of some mobile Na^+ cations in the network arising from the hydrolysis treatment could contribute to increasing osmotic pressure difference between the network and the external solution and enhance hydrophilicity of the corresponding superabsorbent that in turn causes a stronger affinity for more absorption of water.

Besides, all equilibrium swelling ratios of hydrolyzed composites in saline solution are lower compared to those measured in water, irrespective of clay content. Generally, this undesired swelling-loss, commonly observed in the swelling of ionic hydrogels,[50] is often attributed to the charge screening effect of excess Na^+ cations in the swelling media, which shields the carboxylate anions and prevents effective anion-anion electrostatic repulsion. As a result, the osmotic pressure difference between the network and the external medium decreases, and then causes the absorbed water to come out of the hydrogel.

Figure 12 exhibits swelling rates of CTS-*g*-PAAm superabsorbent and one representative MMT composite with 5 wt % MMT loading in water, before and after hydrolysis. It is evident that the rate of water uptake in the hydrolyzed hydrogel is higher than that of unhydrolyzed counterpart. This difference in swelling rate can arises from the presence of hydrophilic COO^- ions in the hydrolyzed hydrogel. It may also be attributed to the particles porosity originating from the hydrolysis. Indeed, during hydrolysis treatment, the reaction mixture becomes pasty and as a result the removed NH_3 and water vapors create

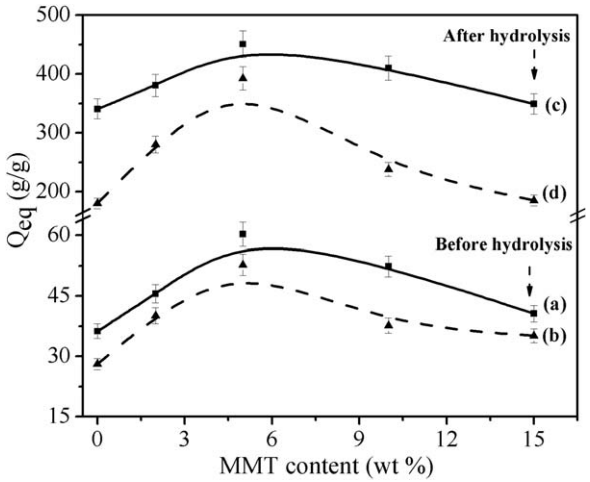

Figure 11. Effects of MMT loading and hydrolysis on water absorbency of the CTS-*g*-PAAm/MMT superabsorbent composites: in doubly distilled water (a) before and (c) after hydrolysis; in 0.9 wt % NaCl (b) before and (d) after hydrolysis.

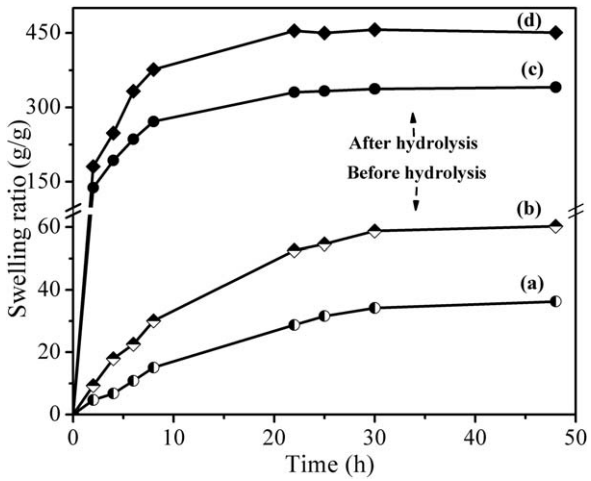

Figure 12. Swelling ratio as a function of time for the superabsorbent CTS-*g*-PAAm (a) before and (c) after hydrolysis as well as for its composite containing 5 wt % of MMT (b) before and (d) after hydrolysis.

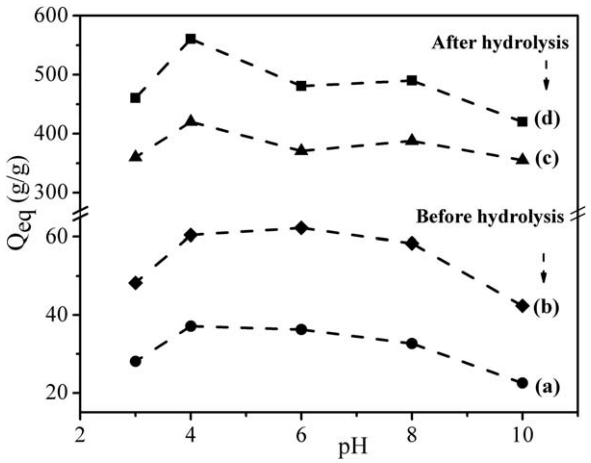

Figure 13. Swelling behavior at various pHs of the superabsorbent CTS-*g*-PAAm (a) before and (c) after hydrolysis as well as for its composite containing 5 wt % of MMT (b) before and (d) after hydrolysis.

additional porosity into the network, which favors subsequent water diffusion through the network.

In the other hand, among the synthesized superabsorbents, the H-CTS-g-PAAm/MMT composite containing 5 wt % of clay shows the highest swelling rate. According to Lee et al.,[51] the initial swelling rate is primarily due to the penetration of water into the network through diffusion and capillarity. The higher initial swelling rate is observed in presence of MMT because the network is relatively loose and the capillarity is more evident, in agreement with above SEM images.

pH-Sensitivity Before and After Hydrolysis

Figure13 displays the pH dependency of the swelling capacity of CTS-*g*-PAAm and a typical superabsorbent composite containing 5 wt % of MMT together with their hydrolyzed analogues, in buffer solutions with pH ranging from 3 to 10. As can be seen, the swelling equilibrium ratios of both CTS-*g*-PAAm and CTS-*g*-PAAm/MMT display pH-sensitivity with similar change trend all through the range of pH investigated, suggesting that the added MMT has no influence on the pH-sensitivity of the matrix. Besides, the swelling capacity of both hydrogels is higher in acid medium than in basic one. It is well known that the swelling of PAAm hydrogel is insensitive to pH value because there are no ionizable groups in this neutral hydrogel. Thus, this result is obviously related to the presence of CTS component that is a weak base with an intrinsic pK_a[52] of 6.5. Under acidic environment, the swelling is controlled mainly by the amino group on the C-2 carbon of the CTS. Indeed, NH_2 groups get protonated and the presence of charge on the CTS backbone enhances the osmotic pressure inside the network owing to NH_3^+- NH_3^+ electrostatic repulsions. This difference in osmotic pressure between the network and the external solution is balanced by the swelling of the hydrogel. In basic region, the ionized NH_3^+groups of CTS change back to NH_2 groups and thus the osmotic pressure decrease. Also at higher pH ~10, the screening effect of ions concentration decreases the difference of osmotic pressure between the network and the medium and thus limits the swelling ability. In neutral medium, the ionic strength is smaller than that in basic media, so provides higher swelling capacity.[53]

Besides, from Figure 13, the swelling behavior of H-CTS-*g*-PAAm and H-CTS-*g*-PAAm/MMT, containing both NH_2 and COO^- groups, changes widely compared to unhydrolyzed counterparts. This result is due to the presence of different interacting species depending on pH medium. As it can be observed, the degree of swelling of both hydrogels is characterized by two maxima at pH 4 and 8. Under acidic pHs ≤ 4, the swelling is promoted mainly by the NH_3^+ species due to the fact that the most of carboxylate ions are protonated (COOH), so that the main anion-anion repulsive forces of COO^- groups are eliminated. Above pH 4, the ionization of carboxylic acid groups occurs since the pK_a of a weak polyacid[54] is about ~4.7, which may enhance the swelling ability. When pH is in the vicinity of 6, the majority of the base and acid groups are as NH_3^+ and COO^- forms, and therefore ionic interaction between these species may lead to ionic crosslinking followed by a decrease in swelling. In basic solution at pH~8, the ionized COO^- groups exerts mutual electrostatic repulsion that causes an expansion of the network chains and hence an increase in swelling. The reason for swelling loss at higher basic solution at pH~10 is once again due to the charge screening effect. Similar results have been reported by other workers.[36,55]

Antibacterial Activity Study

After 24 h of incubation at 37°C, the results of inhibitory zone tests were observed in each sample of Na-MMT, grafted network CTS-*g*-PAAm and its CTS-*g*-PAAm/MMT composites that were swollen in water or acetic acid solution, as are depicted in Figure 14. The MMT shows no inhibitory zones against *E. coli* and *S. aureus*, indicating that these bacteria still grew in the culture plates, so Na-MMT has no antibacterial effect.[56]

All samples swollen in water, images (a,b), show no inhibitory zone against both bacteria, while clear zones around specimens are evidenced in acid medium, images (c,d). These observations are in accordance with previous studies[57,58] on chitosan-based

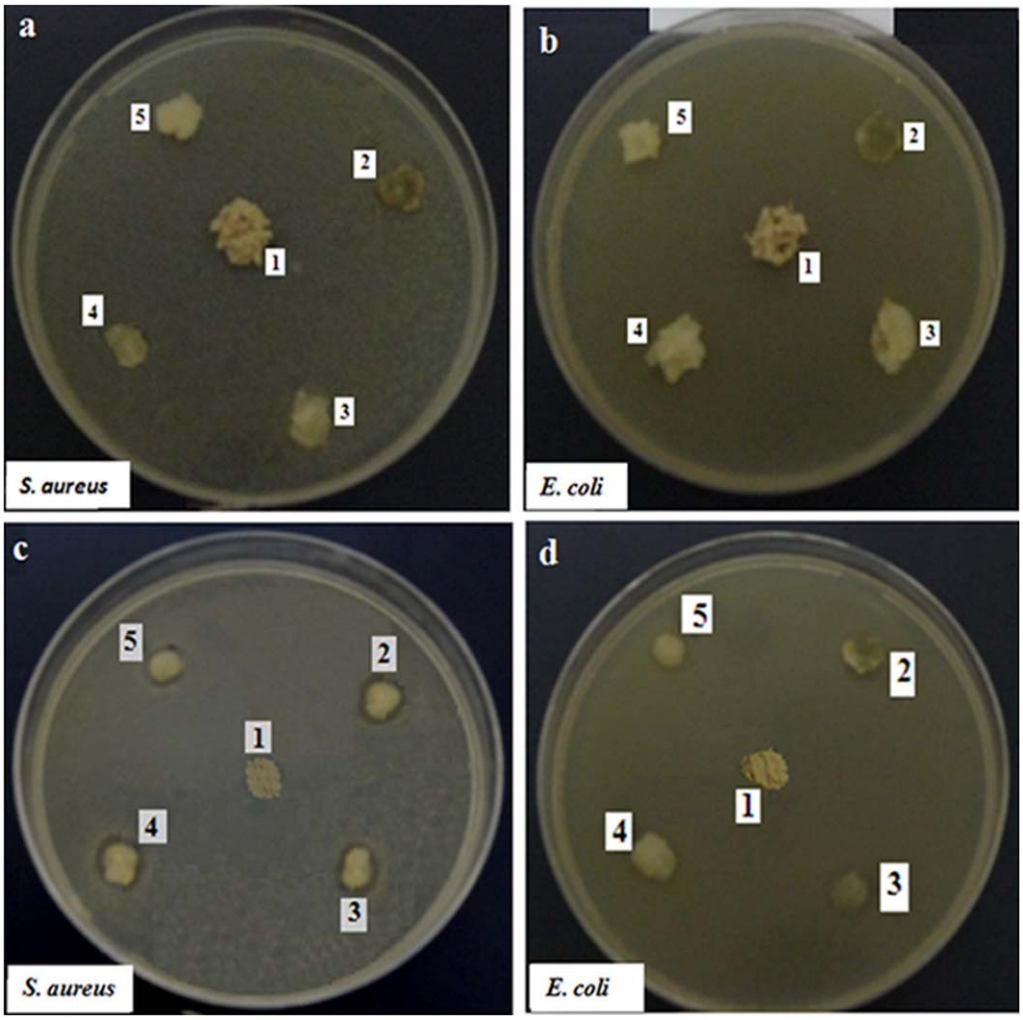

Figure 14. Photographs of antibacterial tests of Na-MMT (1) and superabsorbent composites in distilled water (a,b) and acetic solution (c,d) against *S. aureus* and *E. coli* bacteria; Clay content (wt %): (2) 0%; (3) 5%; (4) 10%; (5) 15%. [Color figure can be viewed in the online issue, which is available at wileyonlinelibrary.com.]

materials. In fact, the antibacterial activity of CTS in acidic environment can originates from its polycationic structure.

The exact mechanism has not been fully elucidated yet, because its activity depends on several factors such as the kind of CTS (deacetylation degree, molecular weight), the pH medium and the temperature. Several mechanism hypotheses have been postulated[59,60]: (1) after the protonation of amino groups NH_2 linking to C-2 on chitosan backbones, the positively charged chitosan $-NH_3^+$ can bind to anionic groups on cell surface and form polyelectrolyte complexes with the bacterial surface compounds thereby disrupt the normal functions of the membrane, e.g., suppressing its biosynthesis, promoting the leakage of intracellular components, inhibiting the transport of nutrients into cells. (2) CTS could chelated with trace elements or essential nutrients, so as to inhibit the growth of bacteria and speeds up their death.

Overall, it also appears from Figure14 that the antibacterial activity of all samples is better against *S. aureus* than *E. coli*. This unlike response towards the Gram-positive and Gram-negative bacteria could be ascribed to morphological differences. Indeed, the structure of the cell wall of Gram-negative strain (*E. coli*) is much complicated than that of Gram-positive strain (*S. aureus*) because there is another layer outside the pepetidoglycan layer called "the outer membrane" that is mainly constructed from tightly packed lipopolysaccharide molecules, resulting in the effective resistive barrier against foreign compounds attack.

Besides, the moderate activity of all hydrogels can be attributed likely to two reasons. The first one is that the antimicrobial activity of CTS is directly related to the number of free amino groups present on it backbone. The probable hydrogen interaction of some NH_2 groups with the carbonyl groups of PAAm give arise to a decrease in free amine groups in the network and subsequently less positive charges, which led to less antibacterial activity of CTS-*g*-PAAm/MMT.[61]The other reason may be related to the solid state of the tested samples. Indeed, the CTS compound exhibits more effective antibacterial ability in dissolved state than in solid one such as in membranes, films and hydrogels systems.

Thus, the superabsorbent composites are found to be active by contact. These materials would be useful in antibacterial applications such as in hygienic products and bio-related uses.

Further quantitative studies on their antibacterial ability against a range of target bacteria using various methods are in progress such as optical density (O.D.) method, which is a test method for determining the antimicrobial activity of materials under dynamic contact conditions.

CONCLUSIONS

Superabsorbent composites were prepared via graft copolymerization of AAm onto CTS backbones in presence of a crosslinker agent and MMT. The grafted network was found thermally more stable than the crosslinked PAAm and CTS and has porous surface. From XRD patterns and SEM images, it was suggested the formation of exfoliated superabsorbent composites with a good dispersion and favorable compatibility of inorganic and organic phases. Also, introducing a small amount of MMT into matrix has generated a loose and more porous surface. Their thermal stabilities could also be enhanced compared to virgin matrix. Besides, all partially hydrolyzed composites, with degree of hydrolysis of ~60%, have shown similar swelling trend than the unhydrolyzed counterparts and behave as excellent superabsorbing materials.

Regardless MMT content, the swelling of hydrogel composites was affected by pH changes and salinity. The hydrolyzed hydrogels composites have exhibited the highest pH sensitivity originating from the ionic repulsion forces between the charged groups of the network. These superabsorbents may be excellent candidates for the design of novel drug delivery systems.

Finally, CTS-*g*-PAAm/MMT superabsorbent composites exhibit moderate antibacterial activity in acidic medium. Also, the sensitivity of *E. coli* was lower compared to that of *S. aureus* that was attributed most likely to the differences in cell wall structure.

This study will be extended to the synthesis of such polymer superabsorbents using several clays and to the investigation of the mechanical properties and the biodegradability of these materials.

ACKNOWLEDGMENTS

The authors are indebted to the applied microbiology laboratory of Bejaia city University (Algeria) and the laboratory of analyze and quality control LAB-DIB in Bejaia city for provision of the research facilities.

REFERENCES

1. Zohuriaan-Mehr, M. J.; Kabiri, K. *Iran. Polym. J.* **2008**, *17*, 451.
2. Buchholz, F. L. *Trends Polym. Sci.* **1994**, *2*, 277.
3. Puoci, F.; Iemma, F.; Spizzirri, U. G. *Am. J. Agric. Biol. Sci.* **2008**, *3*, 299.
4. Kosemund, K.; Schlatter, H.; Ochsenhirt, J. L.; Krause, E. L.; Marsman, D. S.; Erasala, G. N. *Regul. Toxicol. Pharm.* **2009**, *53*, 81.
5. Pourjavadi, A.; Jahromi, P. E.; Seidi, F.; Salimi, H. *Carbohydr. Polym.* **2010**, *79*, 933.
6. Chang, C. Y.; Duan, B.; Cai, J.; Zhang, L. N. *Eur. Polym. J.* **2010**, *46*, 92.
7. Wang, Q.; Zhang, J. P.; Wang, A. Q. *Carbohydr. Polym.* **2009**, *78*, 731.
8. Kong, M.; Chen, X. G.; Xing, K.; Park, H. J. *Int. J. Food Microbiol.* **2010**, *144*, 51.
9. Mellegard, H.; Strand, S. P.; Christensen, B. E.; Granum, P. E.; Hardy, S. P. *Int. J. Food Microbiol.* **2011**, *148*, 48.
10. Dutkiewicz, J. K. *J. Biomed. Mater. Res. A* **2002**, *63*, 373.
11. Kabiri, K.; Omidian, H.; Zohuriaan-Mehr, M. J.; Doroudiani, S. *Polym. Compos.* **2011**, *32*, 277.
12. Jaiswal, M.; Dinda, A. K.; Gupta, A.; Koul, V. *Biomed. Mater.* **2010**, *5*, 1.
13. Wu, J. H.; Wei, Y. L.; Lin, J. M.; Lin, S. B. *Polym. Int.* **2003**, *52*, 1909.
14. Lin, J. M.; Wu, J. H.; Yang, Z. F.; Pu, M. L. *Macromol. Rapid Commun.* **2001**, *22*, 422.
15. Li, A.; Wang, A. Q.; Chen, J. M. *J. Appl. Polym. Sci.* **2004**, *92*, 1596.
16. Zheng, Y. A.; Li, P.; Zhang, J. P.; Wang, A. Q. *Eur. Polym. J.* **2007**, *43*, 1691.
17. Zhang, F. Q.; Guo, Z. J.; Gao, H.; Li, Y. C.; Ren, L.; Shi, L.; Wang, L. X. *Polym. Bull.* **2005**, *55*, 419.
18. Zheng, Y. A.; Wang, A. Q. *Polym. Compos.* **2009**, *30*, 1138.
19. Mansoori, Y.; Atghia, S. V.; Zamanloo, M. R.; Imanzadeh, G.; Sirousazar, M. *Eur. Polym. J.* **2010**, *46*, 1844.
20. Ratinac, K. R.; Gilbert, R. G.; Ye, L.; Jones, A. S.; Ringer, S. P. *Polymer* **2006**, *47*, 6337.
21. Chiu, Y. C.; Huang, L. N.; Vang, C. M.; Huang, J. F. *Colloid. Surf.* **1990**, *46*, 327.
22. Silverstein, R. M.; Bassler, G. C.; Morril, T. C. Spectrometric Identification of Organic Compounds, 5th ed.; Wiley: New York, **1991**; p 135.
23. Ma, G.; Yang, D.; Kennedy, J. F.; Nie, J. *Carbohydr. Polym.* **2009**, *75*, 390.
24. Zhou, C.; Wu, Q. *Colloid. Surf. B* **2011**, *84*, 155.
25. Xia, Y. Q.; Guo, T. Y.; Song, M. D.; Zhang, B. H.; Zhang, B. L. *Biomacromolecules* **2005**, *6*, 2601.
26. Dragan, E. S.; Perju, M. M.; Dinu, M. V. *Carbohydr. Polym.* **2012**, *88*, 270.
27. Sakurai, K.; Maegawa, T. *Polymer* **2000**, *41*, 7051.
28. Pourjavadi, A.; Ayyari, M.; Amini-Fazl, M. S. *Eur. Polym. J.* **2008**, *44*, 1209.
29. Bao, Y.; Ma, J.; Li, N. *Carbohydr. Polym.* **2011**, *84*, 76.
30. Patel, H. A.; Somani, R. S.; Bajaj, H. C.; Jasra, R. V. *Appl. Clay Sci.* **2007**, *35*, 194.
31. Zhang, J.; Wang, L.; Wang, A. *Ind. Eng. Chem. Res.* **2007**, *46*, 2497.

32. Zhang, J.; Wang, Q.; Wang, A. *Carbohydr. Polym.* **2007**, *68*, 367.
33. Xie, Y. T.; Wang, A. Q. *Iran. Polym. J.* **2010**, *19*, 131.
34. Uthirakumar, P.; Nahm, K. S.; Hahn, Y. B.; Lee, Y. S. *Eur. Polym. J.* **2004**, *40*, 2437.
35. Zhao, Q.; Sun, J.; Lin, Y.; Zhou, Q. *React. Funct. Polym.* **2010**, *70*, 602.
36. Pourjavadi, A.; Mahdavinia, G. R. *Turk. J. Chem.* **2006**, *30*, 595.
37. Deng, Y.; Dixon, J. B.; White, G. N.; Loeppert, R. H.; Juo, A. S. R. *Colloid. Surf. A* **2006**, *28*, 82.
38. Zhang, J. P.; Wang, A. Q. *React. Funct. Polym.* **2007**, *67*, 737.
39. Wang, X. Y.; Du, Y. M.; Yang, J. H.; Wang, X. H.; Shi, X. W.; Hu, Y. *Polymer* **2006**, *47*, 6738.
40. Liu, J.; Wang, A. *J. Appl. Polym. Sci.* **2008**, *110*, 678.
41. Darder, M.; Colilla, M.; Ruiz-Hitzky, E. *Appl. Clay Sci.* **2005**, *28*, 199.
42. Chen, Y.; Liu, Y.; Tan, H. *Bioresources* **2008**, *3*, 247.
43. Kabiri, K.; Omidian, H.; Zohuriaan-Mehr, M. *J. Polym. Int.* **2003**, *52*, 1158.
44. Alexandre, M.; Dubois, P. *Mater. Sci. Eng.* **2000**, *28*, 1.
45. Su, X.; Zhang, G.; Xu, K.; Wang, J.; Song, C.; Wang, P. *Polym. Bull.* **2008**, *60*, 69.
46. Li, P.; Zhang, J.; Wang, A. *Macromol. Mater. Eng.* **2007**, *292*, 962.
47. Xie, Y.; Wang, A. *J. Polym. Res.* **2009**, *16*, 143.
48. Zhang, J. P.; Chen, H.; Wang, A. Q. *Eur. Polym. J.* **2005**, *41*, 2434.
49. Peppas, N. A.; Bures, P.; Leobandung, W.; Ichikawa, H. *Eur. J. Pharm. Biopharm.* **2000**, *50*, 27.
50. Castel, D.; Ricard, A.; Audebert, R. *J. Appl. Polym. Sci.* **1990**, *39*, 11.
51. Lee, W. F.; Wu, R. J. *J. Appl. Polym. Sci.* **1996**, *62*, 1099.
52. Kost, J. Encyclopedia of Controlled Drug Delivery; Wiley: New York, **1999**; Vol. *1*.
53. Lárez, C.; Canelón, F.; Millán, E.; Katime, I. *Polym. Bull.* **2002**, *48*, 361.
54. Kiatkamjornwong, S.; Wararuk, C.; Manit, S. *Radiat. Phys. Chem.* **2000**, *59*, 413.
55. El-Sayed, M.; Sorour, M.; Abd-El-Moneem, N.; Talaat, H.; Shalaan, H.; El-Marsafy, N. *World Appl. Sci. J.* **2011**, *13*, 360.
56. Meng, N.; Zhou, N. L.; Zhang, S. Q.; Shen, J. *Int. J. Pharm.* **2009**, *382*, 45.
57. Chung, Y. C.; Wang, H. L.; Chen, Y. M.; Li, S. L. *Bioresource Technol.* **2003**, *88*, 179.
58. Qi, L.; Xu, Z.; Jiang, X.; Hu, C.; Zou, X. *Carbohydr. Res.* **2004**, *339*, 2693.
59. Wu, H. D.; Ji, D. Y.; Chang, W. J.; Yang, J. C.; Lee, S. Y. *Mater. Sci. Eng. C* **2012**, *32*, 207.
60. Yu, Q.; Song, Y.; Shi, X.; Xu, C.; Bin, Y. *Carbohydr. Polym.* **2011**, *84*, 465.
61. Deng, C. M.; He, L. Z.; Zhao, M.; Yang, D.; Liu, Y. *Carbohydr. Polym.* **2007**, *69*, 583.